ELSEVIER

Thermochimica Acta 267 (1995) 181–194

thermochimica acta

Crystallization kinetics of zirconia-yttria gels[1]

J. Málek[2], S. Matsuda, A. Watanabe, T. Ikegami, T. Mitsuhashi*

National Institute for Research in Inorganic Materials, Namiki 1-1, Tsukuba 305, Japan

Received 5 December 1994; accepted 13 February 1995

Abstract

The crystallization kinetics of ZrO_2–Y_2O_3 (3 mol%) dried gels prepared by four different methods was studied by differential scanning calorimetry. It was found that the Johnson–Mehl–Avrami model cannot be used for the description of crystallization of tetragonal zirconia crystals formed in the gel. It was established that this crystallization process can be described by the empirical Šestak–Berggren equation. The influence of the method of preparation is discussed.

Keywords: Zirconia-yttria gels; Crystallization kinetics; DSC

1. Introduction

Ultrafine zirconia (ZrO_2) powder is an important raw material, which has attracted a great deal of attention for use in toughened and high strength ceramics [1,2]. The incorporation of alloying oxides such as Y_2O_3 decreases transition temperatures and also the thermal expansion coefficient which contributes to the better thermal shock resistance of the resulting ceramic material [3].

Precipitation of hydrous zirconia gel and its controlled crystallization is a simple method for the preparation of ultrafine zirconia powders. It is well known that the metastable tetragonal polymorph crystallizes during the heating of zirconia gel [4–8] even though the monoclinic phase is thermodynamically the stable phase at low temperatures. Garvie [9] assumed that this polymorph is formed due to a crystal size effect but later this assumption was critically examined by several authors [10,11]. The crystallization kinet-

* Corresponding author.

[1] Presented at the 30th Anniversary Conference of the Japan Society of Calorimetry and Thermal Analysis, Osaka, Japan, 31 October–2 November 1994.

[2] Permanent address: Joint Laboratory of Solid State Chemistry, Academy of Sciences of the Czech Republic and University of Pardubice, Studentska 84, Pardubice 530 09, Czech Republic.

SSDI 0040-6031 (95) 02477-8

ics of a tetragonal polymorph in zirconia gel was studied by differential thermal analysis (DTA) [12,13] and by hot-stage X-ray diffraction [14]. In these cases the crystallization kinetics was interpreted within the Johnson–Mehl–Avrami model (JMA) [15–18] and the calculated kinetic exponent has been attributed to the dimensionality of crystal growth [12–14]. Unfortunately, the experimental data are not compared directly with the theoretical model and, therefore, it is difficult to verify whether the interpretation is consistent.

The purpose of the present work is a quantitative analysis of the non-isothermal crystallization in dried ZrO_2–Y_2O_3 (3 mol%) gels measured by differential scanning calorimetry (DSC) in order to obtain kinetic parameters characterizing the crystallization process. This composition containing 3 mol% Y_2O_3 typically exhibits very high fracture toughness and high strength of the resulting ceramic material. The gels were prepared by several different methods and the influence of the conditions of gel precipitation on the crystallization kinetics has been studied. A simple method of kinetic analysis [19] allows us to calculate theoretical DSC curves which show very good agreement with the experimental ones.

2. Theory

Usually it is assumed that the heat flow, ϕ, generated during the crystallization process, and measured by DSC, is directly proportional to the rate of the crystallization process, $(d\alpha/dt)$:

$$\phi = \Delta H \cdot (d\alpha/dt) \tag{1}$$

where ΔH is the enthalpy of the crystallization process. Usually an Arrhenius rate constant: $K(T) = A \exp(-E/RT)$ is assumed [20]. Eq. (1) is then expressed in the following form:

$$\phi = \Delta H \cdot A \exp(-E/RT) f(\alpha) \tag{2}$$

where A is the preexponential factor, E is the activation energy, R is the gas constant and T is the absolute temperature. The function $f(\alpha)$ represents the mathematical expression of the phenomenological kinetic model. The functions most frequently used for the description of crystallization processes [20] are summarized in Table 1.

Table 1
Kinetic models used for the description of the crystallization processes

Model	Symbol	$f(\alpha)$
Johnson-Mehl-Avrami [15–18]	JMA	$n(1-\alpha)[-\ln(1-\alpha)]^{1-1/n}$
Šesták-Berggren [25]	SB	$\alpha^M(1-\alpha)^N$

The JMA model [15–18] is frequently used for the description of non-isothermal DSC data as obtained by the DSC technique. Nevertheless, the JMA model was developed to describe isothermal conditions and it has limited applicability for the complex processes involving nucleation and crystal growth [21–24]. Hence, any quantitative analysis of experimental DSC data should be preceded by a reliable test of the applicability of the JMA model. Such a testing method was described recently [26]. A measured DSC curve can be transformed into the function $z(\alpha)$ just by multiplying the measured heat flow by T^2:

$$z(\alpha) = \phi \cdot T^2 \tag{3}$$

If the maximum of this function, α_p^{∞}, is within the interval $0.62 < \alpha_p^{\infty} < 0.64$ then the DSC data can probably be described within the JMA model. On the other hand if the maximum of the $z(\alpha)$ function is lower than 0.60 or greater than 0.66 then the Šestak–Berggren (SB) empirical model [25] is more appropriate for the description of the experimental DSC data [26,27]. It is very important to point out that this simple testing procedure can be done without needing to know any kinetic parameters.

The aim of a kinetic analysis of crystallization processes is to find the best kinetic model providing the calculation of reliable kinetic parameters A and E, characteristic of a particular crystallization process. It is well known, however, that the kinetic parameters A and E in Eq. (2) are mutually correlated [28,29]. So it is practically impossible to determine all kinetic parameters by conventional non-linear regression algorithms of a single DSC curve. From this point of view it seems reasonable to first calculate the activation energy and then determine the kinetic model by the method described below.

The calculation of activation energy is based on a multiple-scan method in which several measurements performed at different heating rates, β, are needed. A very simple method was proposed by Friedman [30] for nth order reactions. However, it was made clear later [31–33] that this method is applicable to various processes. This extended Friedman method follows from the logarithmic form of Eq. (2):

$$\ln \phi = \ln[\Delta H A f(\alpha)] - \frac{E}{RT} \tag{4}$$

The activation energy is calculated from the slope of the plot of the logarithm of normalized heat flow at a given α versus the reciprocal temperature for different heating rates.

The preexponential term in Eq. (2) can be calculated from the condition for the maximum of the DSC peak [19]:

$$A = -\frac{\beta E}{RT_p^2 f'(\alpha_p)} \exp\left(\frac{E}{RT_p}\right) \tag{5}$$

where $f'(\alpha) = \mathrm{d}f(\alpha)/\mathrm{d}\alpha$ and T_p and α_p are the temperature and fractional extent of crystallization at the maximum of the DSC crystallization peak. Thus the $f(\alpha)$ function is necessary for the calculation of the preexponential factor. The type of kinetic model $f(\alpha)$ can

be determined using the $z(\alpha)$ function as described above. The kinetic exponents n or (M,N) can be calculated provided that the activation energy is known.

For this purpose it is useful to define a function $y(\alpha)$ which can easily be obtained by simple transformation of DSC data [19]:

$$y(\alpha) = \phi \exp(E/RT) \tag{6}$$

The maximum α_m of the $y(\alpha)$ function is confined to the interval: $0 \leq \alpha_m < \alpha_p$. The kinetic exponents for the JMA and SB models can be calculated from the α_m value:

3. The JMA model

If the function $y(\alpha)$ has a maximum at $\alpha_m > 0$ the kinetic exponent n can be calculated using the following equation [19]:

$$n = \frac{1}{1+\ln(1-\alpha_m)} \tag{7}$$

If the maximum of the $y(\alpha)$ function is located at $\alpha_m = 0$ then the parameter n can be calculated by means of Šatava's method [34], from the slope of the plot of $\ln[-\ln(1-\alpha)]$ versus $1/T$ which is nE/R. Another method of calculation of this parameter is based on the relationship derived from the condition for the maximum of the DSC peak [19]:

$$n = \frac{1-x_p\pi(x_p)}{\ln(1-\alpha_p)} \tag{8}$$

The Šatava method usually gives slightly higher values of the kinetic exponent n than Eq. (8). Usually [19], an average of these two values is a good approximation of the kinetic exponent.

4. The SB model

The ratio of the kinetic exponents M/N can be calculated from the maximum of the $y(\alpha)$ function [19]:

$$\frac{M}{N} = \frac{\alpha_m}{1-\alpha_m} \tag{9}$$

Eq. (2) may be written in the following form:

$$\ln[\phi \exp(E/RT)] = \ln(\Delta H \cdot A) + N \ln[(\alpha^{M/N}(1-\alpha)] \tag{10}$$

The kinetic parameter N is then calculated [19] from the slope of the linear dependence of $\ln[\phi \exp(E/RT)]$ versus $\ln[\alpha^{M/N}(1-\alpha)]$ plotted in the interval $\alpha \in (0.2,0.8)$.

The kinetic exponents in the $f(\alpha)$ function are linked with the mechanism of the crystallization process but their direct interpretation in terms of crystal growth morphology can be very problematic. Any conclusions in this respect should be always supported by microscopic observation of the crystallization process or other relevant measurements.

5. Experimental

The samples of ZrO_2-Y_2O_3 (3 mol%) gels were prepared by four different methods from 0.1 M Zr^{4+} and Y^{3+} solutions:

(A) conventional co-precipitation method using NH_4OH;
(B) masking of Zr^{4+} by H_2O_2, adding Y^{3+} solution and then co-precipitation by urea at 70–100°C;
(C) masking of Zr^{4+} by H_2O_2, adding Y^{3+} solution with urea, pH control by NH_4OH, and then co-precipitation by $(NH_4)_2SO_4$;
(D) masking of Zr^{4+} by H_2O_2, adding Y^{3+} solution and co-precipitation by NH_4OH.

The voluminous gels obtained were washed five times in distilled water, filtered and dried in a vacuum at room temperature for 3 days and then they were grounded with agate mortar.

The powder X-ray diffraction (XRD) investigations of the prepared samples were conducted using Ni-filtered $Cu_{K\alpha}$ radiation (Model PW-1130, Phillips). The XRD patterns of the as-received samples (A)–(D) exhibit a broad halo with a maximum which corresponds to the interplanar spacing of cubic (1 1 1). The morphology of dried gels was examined by scanning electron microscopy (SEM) (Model S5000, Hitachi). Thermogravimetric (TG) experiments were carried out in a nitrogen atmosphere using about 20 mg sample (Model TGA7, Perkin-Elmer). Simultaneous thermogravimetric and mass spectroscopy measurements (TG-MS) were carried out in a helium atmosphere (Model TG-DTA-MS, Rigaku).

Differential scanning calorimetry (DSC) measurements of the crystallization kinetics were carried out in an atmosphere of dry nitrogen on samples of about 10 mg in aluminum sample pans (Model DSC-7, Perkin-Elmer). The instrument was previously calibrated with In, Pb, and Zn standards. Non-isothermal DSC curves were obtained with selected heating rates 2–20 K min^{-1} in the range 25–600°C. The kinetic analysis of the DSC data and all calculations were performed by the TA-SYSTEM software package [19].

6. Results and discussion

Typical TG curves for ZrO_2–Y_2O_3 (3 mol%) gels prepared by the four different methods, measured with a nitrogen flow and heating rate of 5 K min^{-1}, are shown in Fig. 1a. The differential thermogravimetric (DTG) curves for the same samples under the same conditions are illustrated in Fig. 1b. The behavior of samples A, C and D are similar, with the greatest weight loss being for temperatures up to 250°C. The final weight loss is

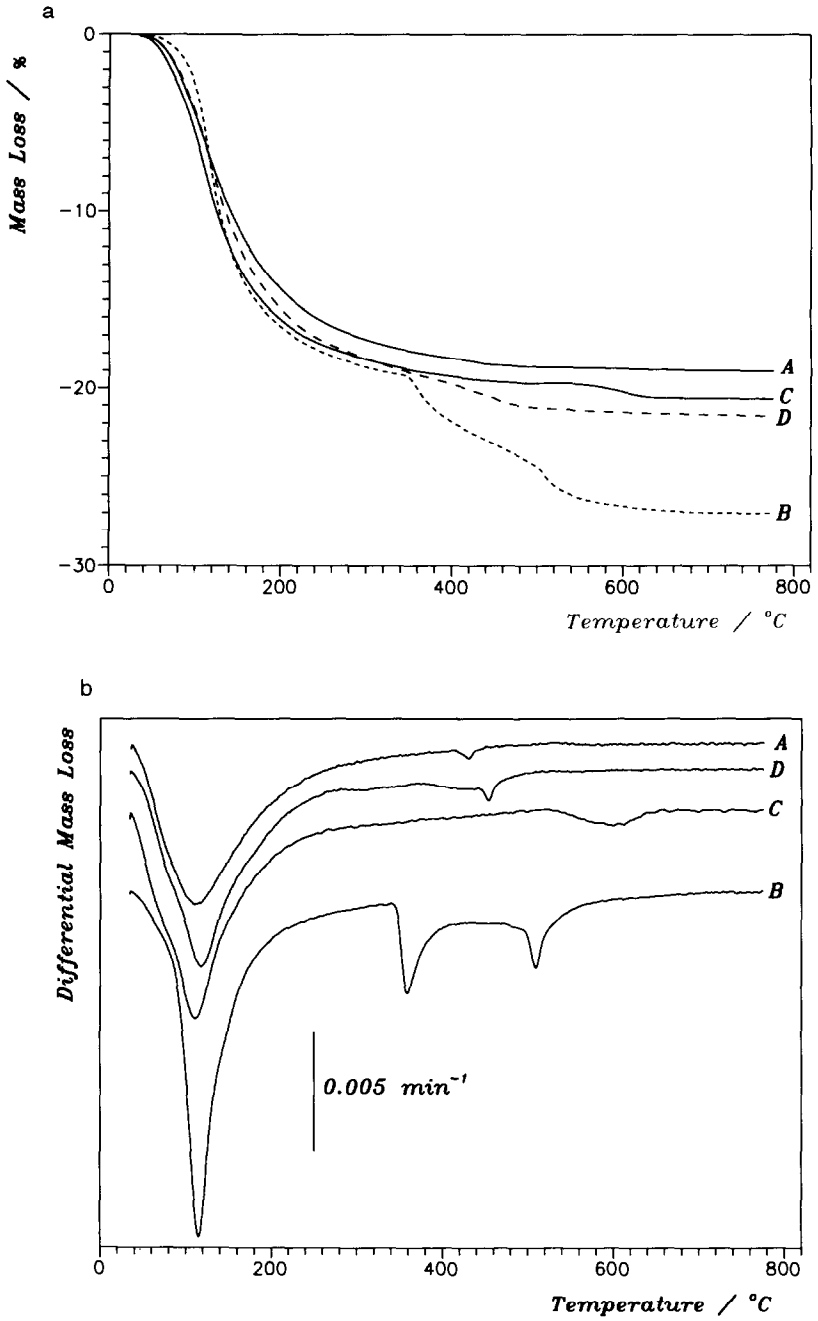

Fig. 1. (a) Typical TG curves for ZrO_2–Y_2O_3 (3 mol%) gels prepared by methods A, B, C and D. Curves measured with nitrogen gas flow of 10 ml min^{-1} at a heating rate 5 K min^{-1}. (b) Calculated differential DTG curves for the same samples.

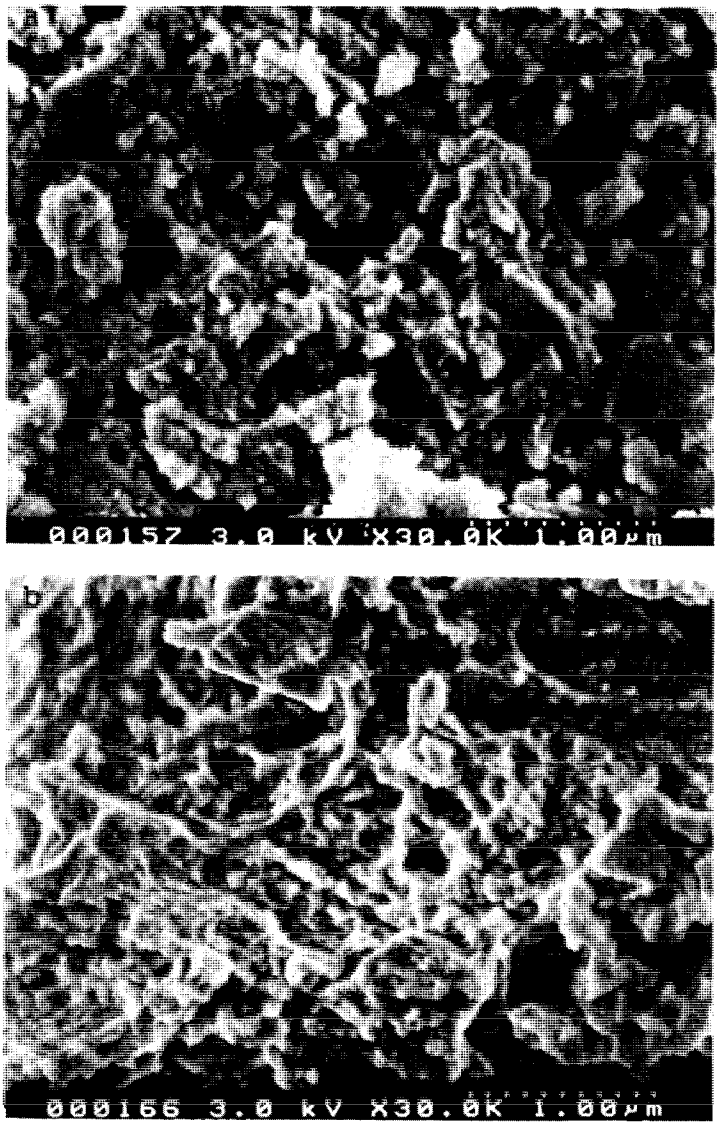

Fig. 2. SEM micrograph of as-received ZrO_2–Y_2O_3 (3 mol%) gels. (a) Sample A, (b) Sample B.

about 20% of the initial sample weight, being attained after heating to 400°C. The DTG curves (Fig. 1b) show a sharp maximum at approximately 115°C which can probably be associated with the loss of adsorbed water. The rate of the mass loss at this maximum is comparable for samples A, C and D (Fig. 1b). In contrast, sample B exhibits nearly two times higher rate of mass loss at the maximum and also the final weight loss is higher, i.e. 27%. There are also two other DTG peaks in the range 300–600°C for sample B and one

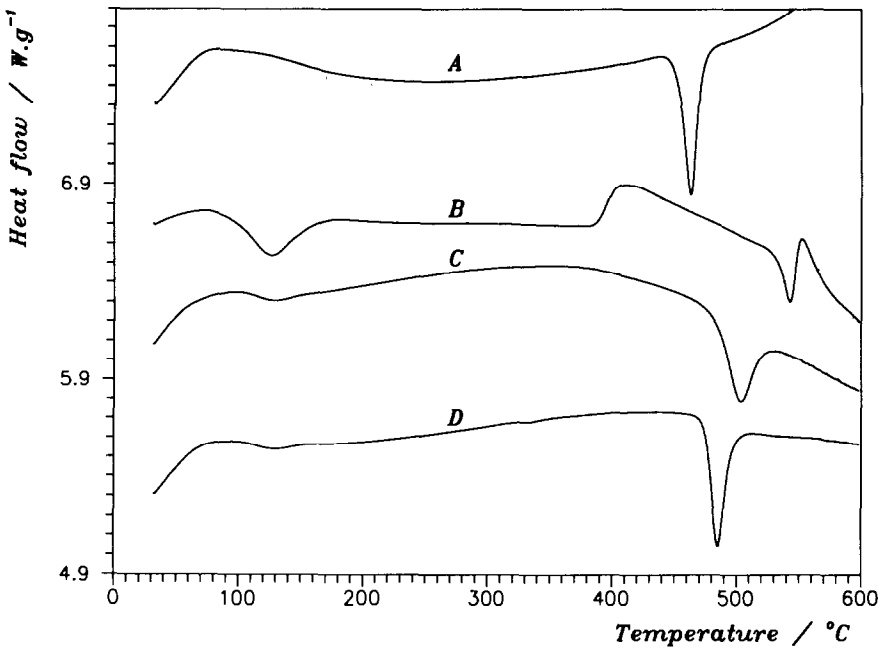

Fig. 3. Typical DSC curves for ZrO_2–Y_2O_3 (3 mol%) gels prepared by methods A, B, C and D. Curves measured for a nitrogen gas flow of 10 ml min^{-1} at a heating rate 5 K min^{-1}.

broader peak at about 600°C for sample C. These peaks can probably be attributed to decomposition of urea traces, as suggested by TG-MS measurements.

Typical structures of prepared ZrO_2–Y_2O3 (3 mol%) gels can be seen in Fig. 2. The SEM micrographs are very similar for samples A, C and D. Small particles (about 0.1 μm) form more complex agglomerate grain structures with varying degrees of porosity (Fig. 2a). Sample B (Fig. 2b) exhibits a more closed structure with a smoother surface where the grains are bridged together. This is probably one of the reasons why sample B exhibits a different TG behavior in comparison with samples A, C and D. The DSC curves for four samples of yttria containing zirconia gels, measured with a nitrogen flow and heating rate of 5 K min^{-1}, are shown in Fig. 3. All these curves exhibit a broad endothermic peak at about 120°C, being probably associated with the loss of adsorbed water from the gel. A characteristic feature of all the DSC curves in Fig. 3 is the sharp exothermic peak observed in the range 450–600°C corresponding to crystallization of dried gel. The average enthalpies of crystallization, ΔH_c, were determined for all four samples and are summarized in Table 2. The ΔH_c values are very close for samples C and D, but about 20% higher for sample A and about 40% lower for sample B. Smaller ΔH_c value observed for sample B can probably be explained as a consequence of overlapping of the crystallization process and endothermic mass loss. The crystallization occurs after the residual water is removed from the sample as evident from a comparison of Figs. 1b and 3. The XRD analysis of the samples after DSC measurement shows that a tetragonal zir-

Table 2
The kinetic parameters of crystallization process

Sample	$-\Delta H$/J g^{-1}	E/kJ mol^{-1}	M	N	ln[$A(s^{-1})$]
A	124 ± 13	285 ± 5	1.13 ± 0.03	1.4 ± 0.1	43.30 ± 0.07
B	60 ± 7	285 ± 5	0.5 ± 0.1	0.3 ± 0.1	38.5 ± 0.2
C	102 ± 5	327 ± 2	0.66 ± 0.05	1.39 ± 0.08	46.5 ± 0.1
D	104 ± 3	312 ± 5	0.86 ± 0.05	1.44 ± 0.01	46.0 ± 0.1

conia phase is formed during the crystallization process. This was also confirmed by Raman spectroscopy using the method described in Ref. [35].

The crystallization process can be followed by non-isothermal DSC measurements taken at different heating rates and later analyzed by the method described above. The samples of yttria containing zirconia gels were measured by DSC using five different heating rates: 2, 5, 10, 15 and 20 K min^{-1}. The dependence of the activation energy of the crystallization process on α, determined using Eq. (4) is shown in Fig. 4 (full lines). The average values of the activation energy determined in the restricted range $0.3 < \alpha < 0.7$ are shown by broken lines and summarized in Table 2. These values were used for the kinetic calculations. The variation of E versus α is within 10% for samples C and D but it is higher for samples A and B.

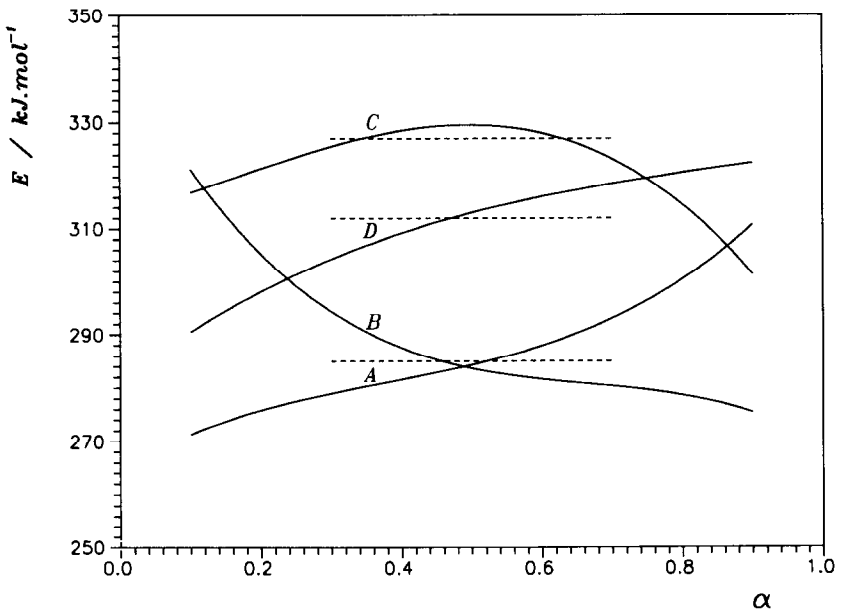

Fig. 4. Activation energies, E, at various fractional extent of crystallization α (full lines), calculated from DSC data (using Eq. (4)) for ZrO_2–Y_2O_3 (3 mol%) gels prepared by methods A, B, C and D. The broken lines show the average E value in the restricted interval $0.3 < \alpha < 0.7$, used for kinetic calculations.

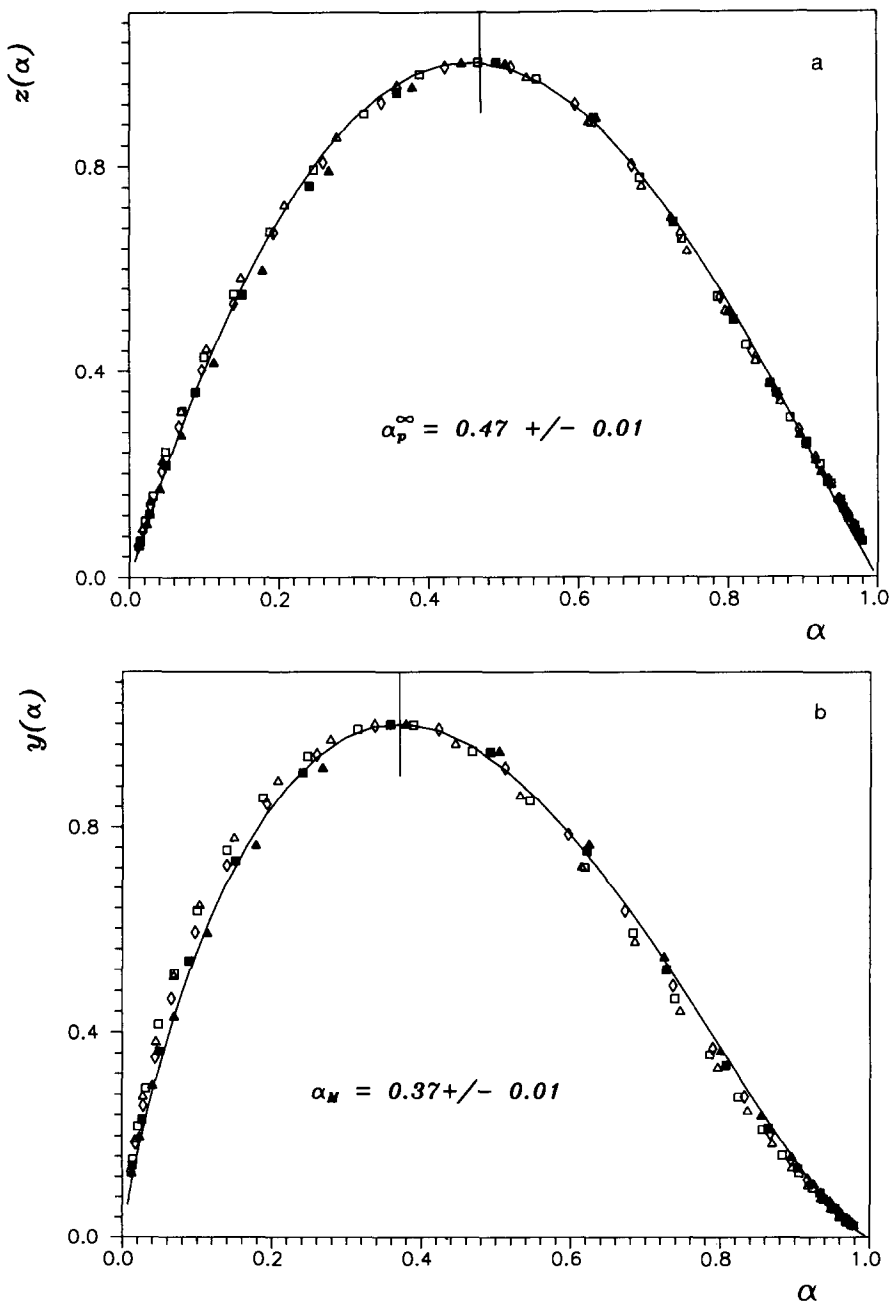

Fig. 5. (a) Normalized $z(\alpha)$function. (b) Normalized $y(\alpha)$ function calculated from the DSC data for ZrO_2–Y_2O_3 (3 mol%) gel prepared by method D. The heating rates are shown by various points: □, 2.5; △, 5; ◇, 10; ■,15 and ▲, 20 K min^{-1}. The points were calculated by Eqs. (3) and (6), and the full lines correspond to $\{[df(\alpha)/d\alpha]/d\alpha/f(\alpha)]\}$ and $f(\alpha)$ functions.

Table 3
The maxima of the $y(\alpha)$ and the $z(\alpha)$ function

Sample	α_m	α_p^∞
A	0.44 ± 0.01	0.53 ± 0.01
B	0.61 ± 0.03	0.69 ± 0.03
C	0.32 ± 0.01	0.50 ± 0.01
D	0.37 ± 0.01	0.47 ± 0.01

Experimental DSC data can be converted to the $z(\alpha)$ and $y(\alpha)$ functions using Eqs. (3) and (6). These two functions, normalized within a (0,1) interval, corresponding to sample D are shown in Fig. 5 for different heating rates (points). For better clarity, not all the data points are included in this figure. Both these functions are independent of the heating rate and give well-defined maxima. The values of α_p^∞ and α_m corresponding to the maxima are summarized for all samples in Table 3. It is evident that the maximum of the $z(\alpha)$ function is far from the interval $0.62 < \alpha < 0.64$, typical for the JMA model. Therefore, it seems that this model cannot be used for the description of the crystallization process in yttria containing zirconia gels. It is well known that the JMA model was originally derived for the description of transformation processes under isothermal conditions. Its applicability under non-isothermal conditions (e.g. DSC measurements) is limited to some special cases where a new phase grows from a constant number of nuclei. This is

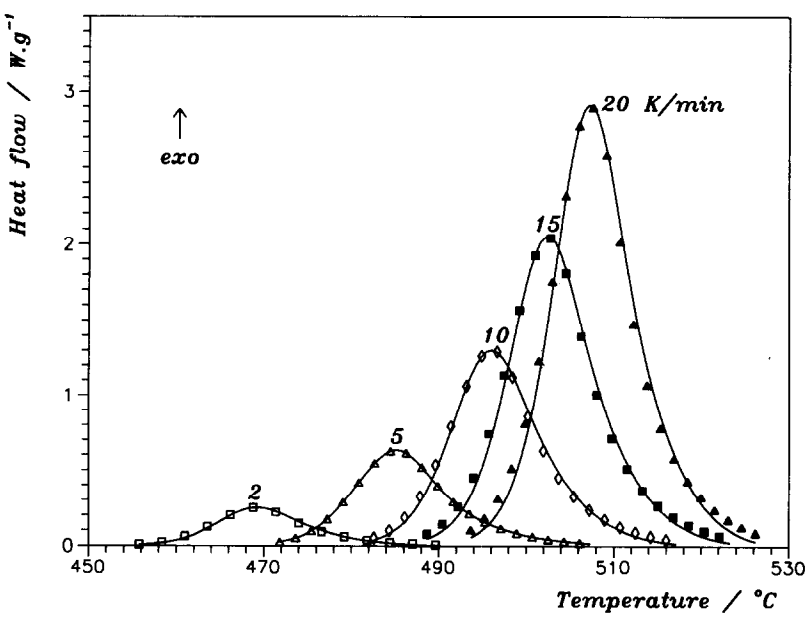

Fig. 6. Experimental (points) and calculated (full lines) DSC curves corresponding to the crystallization at various heating rates of ZrO_2–Y_2O_3 (3 mol%) gel prepared by method D. The symbols used are as in Fig. 4.

equivalent to the situation where all nucleation is completed prior to crystal growth. It seems that this condition is not fulfilled in the case of amorphous zirconia gels. It seems that the nucleation process and the growth of the primary crystallites occur simultaneously after removal of adsorbed water from the sample. In this case the crystallization process can be described by the empirical SB model. The kinetic parameters ln A, M and N, calculated by Eqs. (5), (9) and (10) are summarized in Table 2.

Experimental (points) and calculated DSC curves (full lines) are compared in Fig. 6 for sample D measured at five different heating rates. From a comparison it is apparent that the crystallization process can be well described by the SB model within the error limits indicated in Table 2. The consistency of this model can by verified also by calculation of theoretical $z(\alpha)$ and $y(\alpha)$ functions. By comparing Eqs. (2) and (6) it is evident that the $y(\alpha)$ function is proportional to the obtained $f(\alpha)$ function. Similarly, it can be shown [19] that the $z(\alpha)$ function is proportional to $\{[df(\alpha)/d\alpha]\int d\alpha/f(\alpha)\}$. The $f(\alpha)$ function is defined by the parameters M and N summarized in Table 2. Thus it is possible to calculate theoretical $z(\alpha)$ and $y(\alpha)$ functions as shown by the full lines in Fig. 5. Agreement between these theoretically calculated functions and the experimental data converted by Eqs. (2) and (6) is quite good.

The same analysis was performed also for samples A, B and C. Experimental (points) and calculated DSC curves (full lines) are compared in Fig. 7 for all four samples at a heating rate of 10 K min^{-1}. Samples A and D exhibit sharp DSC peaks corresponding to

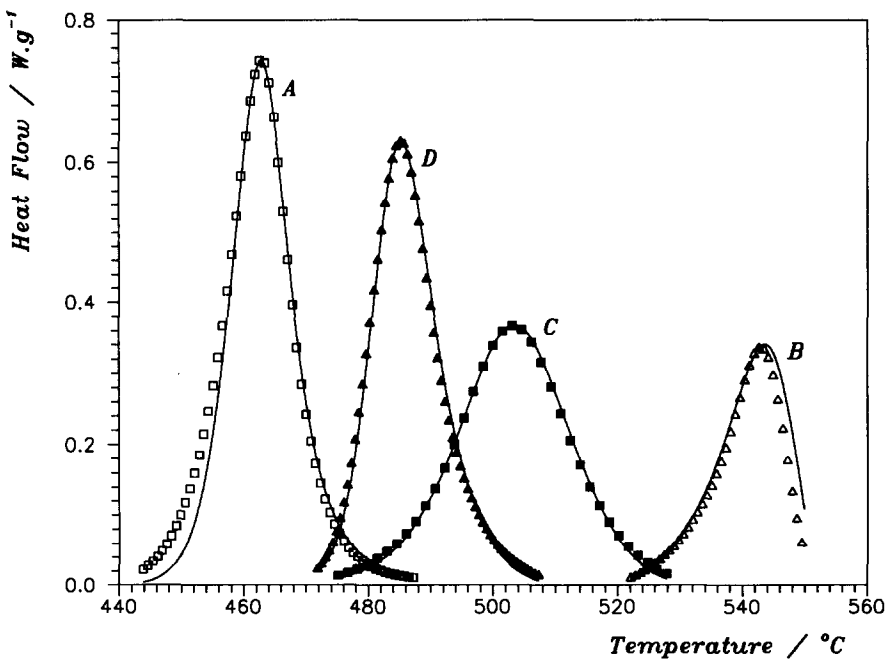

Fig. 7. Experimental (points) and calculated (full lines) DSC curves (heating rate 10 K min^{-1}) corresponding to ZrO_2–Y_2O_3 (3 mol%) gels prepared by methods A, B, C and D.

rapid crystallization. On the other hand the crystallization process in samples B and C took place more gradually. Hence, the DSC peaks are broader and their positions are shifted towards higher temperatures. From the point of view of a quantitative description the best agreement between measured and calculated DSC curves can be found for samples C and D.

7. Conclusion

The samples of dried ZrO_2–Y_2O_3 (3 mol%) gels were prepared by four different methods. The crystallization kinetics were studied by DSC under non-isothermal conditions. The crystallization process is started after adsorbed water has been removed from the sample. It was found that the JMA model cannot be applied for the description of the experimental data. One possible explanation is that both nucleation and crystal growth processes overlap and therefore one of the basic assumptions for the applicability of this model is not fulfilled. It was established, however, that the empirical SB kinetic model gives a good description of DSC data. The results reported here indicate that the method of precipitation used in the preparation of zirconia gels are important factors in crystallization behavior.

Acknowledgements

The authors wish to thank to Dr. M. Yashima for his kind assistance with the Raman spectroscopy. One of the authors (J.M.) expresses his appreciation to the Science and Technology Agency of Japan for financial support.

References

[1] M. Ruhle, N. Claussen and A.H. Heuer, in N. Clausen, M. Ruhle and A.H. Heuer (Eds.), Advances in Ceramics, Vol. 12, The American Ceramic Society, 1984, pp. 352–370.
[2] K. Tsukuma, K. Leda, K. Matsushita and M. Shimada, J. Am. Ceram. Soc., 68 (1985) C56.
[3] E.C. Subbarao, in A.H. Heuer and L.W. Hobbs (Eds.), Advances in Ceramics, Vol. 3, The American Ceramic Society, 1981, pp 1–24.
[4] J. Livage, K. Doi and C. Mazieres, J. Am. Ceram. Soc., 51 (1968) 349.
[5] M.A. Blesa, A.J.G. Maroto, S.I. Passaggio, N.E. Figliolia and G. Rigotti, J. Mater. Sci., 20 (1985) 4601.
[6] G. Cimblett, A.A. Rahman and K.S.W. Sing, J. Chem. Tech. Biotechnol., 30 (1980) 51–64.
[7] Ph. Colomban and E. Bruneton, J. Non-Cryst. Solids, 147,148 (1992) 201–205.
[8] J.C. Debsikdar, J. Non-Cryst. Solids, 86 (1986) 231.
[9] R.C. Garvie, J. Phys. Chem., 69 (1965) 1238.
[10] T. Mitsuhashi, M. Ichihara and U. Tatsuke, J. Am. Ceram. Soc., 57 (1974) 97–101.
[11] R. Srinivasan, L. Rice and B.H. Davis, J. Am. Ceram. Soc., 73 (1990) 3528.
[12] T. Mitsuhashi, in NIRIM Report No. 7, National Institute for Research in Inorganic Materials, 1974, pp. 17–31.
[13] A. Aronne, P. Pernice and A. Marotta, J. Mater. Sci. Lett., 10 (1991) 1136.
[14] S. Ramanathan, N.C. Soni and R. Prasad, J. Mater. Sci. Lett., 12 (1993) 122.
[15] W.A. Johnson and R.F. Mehl, Trans. Am. Inst. Min. Eng., 135 (1939) 416.

[16] M. Avrami, J. Phys. Chem., 7 (1939) 1103.
[17] M. Avrami, J. Phys. Chem., 8 (1940) 212.
[18] M. Avrami, J. Phys. Chem., 9 (1941) 177.
[19] J. Málek, Thermochim. Acta, 200 (1992) 257.
[20] J. Šesták, Thermophysical Properties of Solids, Their Measurements and Theoretical Analysis, Elsevier Amsterdam, 1984.
[21] D.W. Henderson, J. Therm. Anal., 15 (1979) 325.
[22] D.W. Henderson, J. Non-Cryst. Solids, 30 (1979) 301.
[23] T.J.W. DeBruijn, W.A. DeJong and P.J. Van Den Berg, Thermochim. Acta, 45 (1981) 315.
[24] H. Yinnon and D.R. Uhlmann, J. Non-Cryst. Solids, 54 (1983) 253.
[25] J. Šesták and G. Berggren, Thermochim. Acta, 3 (1971) 1.
[26] J. Málek, Thermochim. Acta, Thermochim. Acta, 267 (1995) 61.
[27] J. Málek and V. Smrčka, Thermochim. Acta, 186 (1991) 153.
[28] N. Koga, J. Šesták and J. Málek, Thermochim. Acta, 188 (1991) 333.
[29] J. Málek and J.M. Criado, Thermochim. Acta, 203 (1992) 25.
[30] H.L. Friedman, J. Polym. Sci., C6 (1964)183.
[31] T. Ozawa, Thermochim. Acta, 31(1986) 547.
[32] T. Ozawa, Thermochim. Acta, 203 (1992)159.
[33] J.H. Flynn and L.A. Wall, J. Polym. Sci., B4 (1966) 323.
[34] V. Satava, Thermochim. Acta, 2 (1971) 423.
[35] M. Yashima, K. Ohtake, H. Arashi, M. Kakihana and M. Yoshimura, J. Appl. Phys., 74 (1993) 7603.